

SOIL MICROMORPHOLOGY, CHEMISTRY AND MAGNETIC SUSCEPTIBILITY STUDIES AT HUIZUI (YILUO REGION, HENAN PROVINCE, NORTHERN CHINA), WITH SPECIAL FOCUS ON A TYPICAL YANGSHAO FLOOR SEQUENCE

Richard I. Macphail¹ and John Crowther²

¹Institute of Archaeology, University College London, 31-34, Gordon Sq, London, WC1H 0PY, UK

²Department of Archaeology & Anthropology, University of Wales, Lampeter, Ceredigion, SA48 7ED, UK

Email: r.macphail@btopenworld.com

Keywords: China, Huizui, geoarchaeology, chemistry, magnetic susceptibility

ABSTRACT

31 thin sections and 25 bulk samples were investigated from Huizui (Loess Plateau of northern China) creating a broad, albeit limited, dataset for the Peiligang, Yangshao, Longshan and Erlitou Periods. The study provides punctuated insights into the occupational and landscape history of the site. These are briefly reported in order to examine, in context, some details of a typical Yangshao Peiligang floor sequence (11 layers). Here, ground-raising was achieved mainly through constructing layers of plant-tempered adobe, manufactured from 'clean' loess that is present at Huizui. A dark, 'red' coloured mud-plastered surface was made at the top of the adobe layers, to underlie each 'white' floor. Contrary to expectation, soil micromorphology found that the 'white' floors are not 'burned lime' floors, but single and multiple quarried slabs of fossiliferous tabular formed tufa, of likely Quaternary age and local origin; a finding consistent with bulk analyses. As these slabs appear to be at least 3-4 m in size their quarrying and transport imply a high degree of social organization. No Yangshao occupation floor deposits were found, suggesting that either floors were of ritual use or were swept or mat-covered. An example of an off-site gleyed, Yangshao to Longshan soil-sediment sequence, containing anthropogenic inclusions, was found to overlie the local truncated grey, gleyed, and archaeologically sterile Late Pleistocene/Early Holocene alluvial soil.

INTRODUCTION

During 2005, two archaeological fieldwork seasons in and around Huizui, Yiluo Region, Henan Province, China, led to the microstratigraphic analysis of geoarchaeological samples from the Peiligang, Yangshao, Longshan and Erlitou Periods (see Samples and methods; Table 1 after main text; Map 1 for site locations). This microstratigraphic study is a recent component of the interdisciplinary Yiluo Project (2003-2006), investigating geoarchaeology, plant remains, settlement patterns, craft specialization, and the rise of Chinese civilization on this part of the

Loess Plateau (Liu *et al.* 2002-2004). Analysis of microstratigraphy at Huizui, employing the techniques of soil micromorphology, chemistry and magnetic susceptibility, had the aims of characterizing the natural soils and sediments of the locality in order to identify occupation deposits, such as ash pit fills, 'white' floor sequences, and selected contexts of an enigmatic near-river soil-sediment accumulation. This paper mainly focuses upon a typical Yangshao floor sequence and several ash pits (Map 2 for sampling locations). Preliminary interpretations of other deposits are also given, in order to understand more accurately the Yangshao floor sequence, within its archaeological and landscape context.

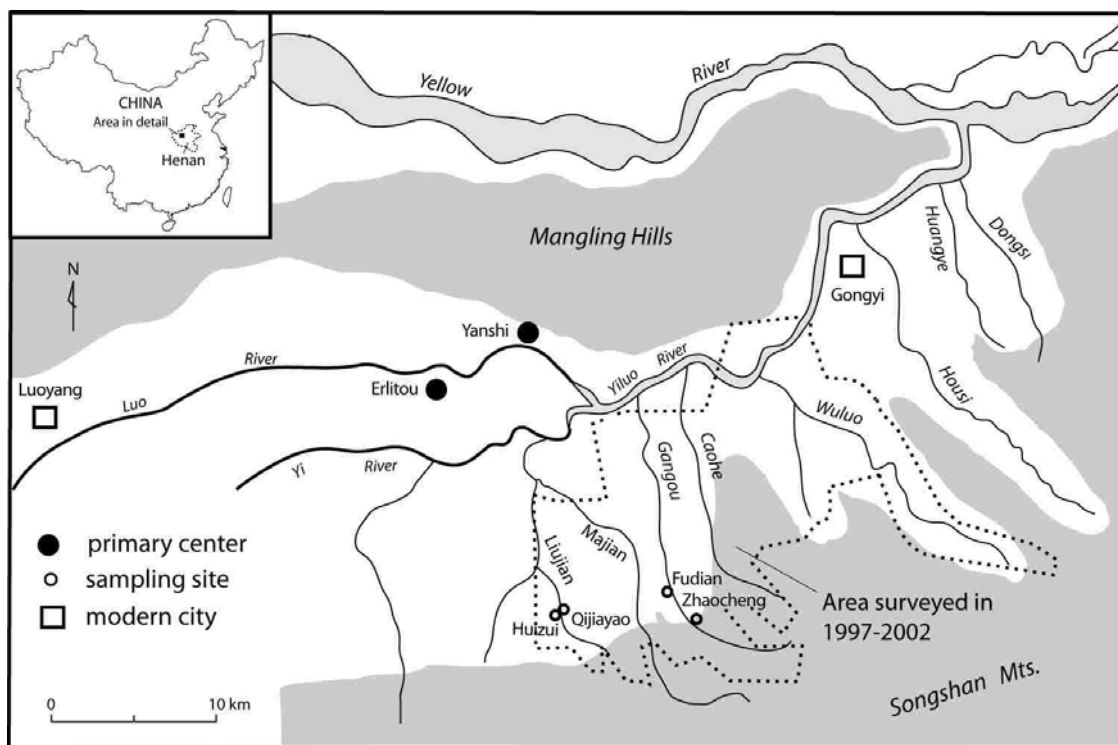
SAMPLES AND METHODS

A selection of samples collected early in 2005 by Chen (Institute of Archaeology, Chinese Academy of Social Sciences, China) were received at UCL and assessed through soil micromorphology (the study of undisturbed soils and sediments in 20-30 μm thick thin sections; Courty *et al.* 1989) and bulk analyses (see below). This aided the sampling strategy of the Yiluo Project team that included Macphail during fieldwork carried out in November 2005.

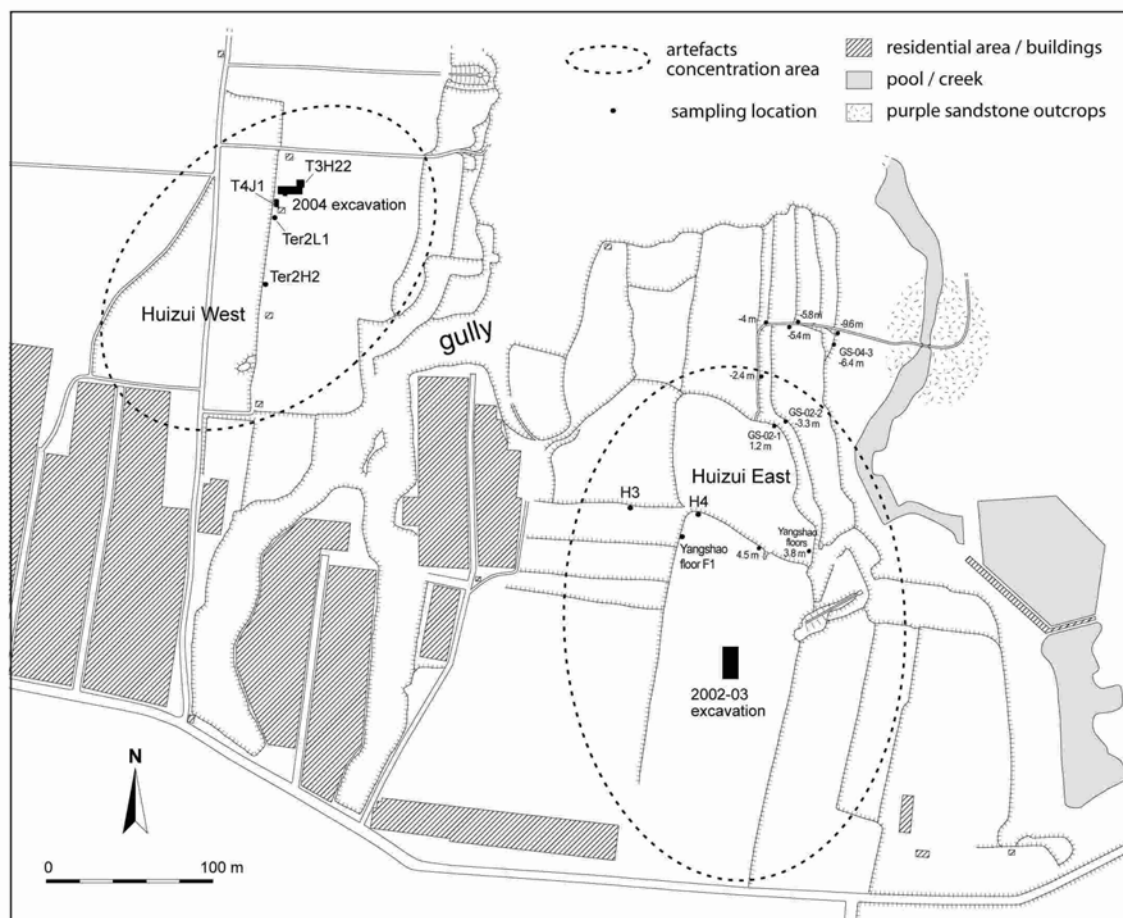
In all, 44 undisturbed monolith (Figure 1) and 37 bulk samples were available for study. Discussion with co-workers led to the selective investigation of 31 thin sections and 25 bulk samples (Table 1), in order to answer selected archaeological questions.

The microstratigraphic approach

Full details of the methods applied are given elsewhere (Goldberg and Macphail 2006; Macphail and Crowther 2004). Essentially, soil micromorphology (which included microprobe X-ray analysis), was combined with the bulk measurements of loss-on-ignition (LOI at 375°C), fractionated phosphate (inorganic and organic P), magnetic susceptibility (including $\% \chi_{\text{conv}}$) and the heavy metals copper (Cu), lead (Pb) and zinc (Zn) (Bethell and Máté 1989; Courty *et al.* 1989; Crowther 2003; Crowther and Barker 1995; Stoops 2003).



Map 1: The Yiluo Project: site locations.



Map 2: Sampling locations at Huizui.

RESULTS AND DISCUSSION

Selected results are presented in Tables 1-2 and Figures 1-9, including a preliminary interpretation of each context studied (Table 1).

Post-deposition effects

The soil and landscape at and around Huizui has been highly manipulated by human populations for millennia. A Late Pleistocene/early Holocene alluvial soil (sample 40) at GS2 is considered a good example of a sterile ‘control’ sample. As would be expected, this ‘natural’ soil has a relatively low LOI (organic content), a low phosphate concentration and a very low magnetic susceptibility; its chief characteristics are a massive structure and iron stained porosity (relict root channels) typical of alluvial gley soils (Bouma *et al.* 1990). This soil has also been affected by later secondary calcium carbonate formation. The latter is believed to be the result of a general contamination of archaeological soils by calcium carbonate and other alkaline salts, which have produced anomalously high pH values (max. pH 9.6) across the site (see Table 2); all possibly linked to alkaline occupational deposits that were markedly present at Huizui at least since the Yangshao Period (see below). The effects of burrowing by fauna such as insects and small mammals has also to be considered (see Layer 11, Figure 1).



Figure 1: Huizui Yangshao F1 floor sequences 05HYEHF1 (see Rosen, this volume: Figure 2); ground-raising and preparation surfaces (Layers 1, 3, 5, and 7), floors (Layers 2, 4, 6 and 8) and burned daub (adobe) debris (Layer 9); samples M16-M19. Note biologically worked and homogenised upper deposits (Layer 11) and possible vertical wall or partition (white arrow).

Local soils

Field and soil micromorphological observations of soils at Qijiayao (Peiligang pits; sample 43) and in soils below a Yangshao pit at Huizui (sample M32) indicate the typical presence of iron- and clay-depleted upper subsoil A2 horizons and the relatively more clay- and iron-rich lower subsoil Bw/B(t) horizons formed in silty clay loam loess under a broad-leaved woodland. These lower subsoils also

often contain secondary calcium carbonate (B(t)k /Ck horizons), and at Zhaocheng, Pleistocene palaeosols are characterised by marked carbonate nodular formation. This is typical of Holocene (and earlier) pedogenesis on loess, predominantly a wind blown silt (Duchaufour, 1982: 233-4, 282), with leaching and clay migration, and secondary carbonate formation at depth, forming a *Hapludalf* (Soil Survey Staff 1999) or *Orthic (Calcic) Luvisol* (FAO-Unesco 1988).



Figure 2: Scan of 15 cm long impregnated block (M18) that sampled Layer 5 – a plant-tempered adobe preparation surface (APS), and Layer 6 – a series of fossiliferous tufa floor layers (TFL) composed of quarried slabs of tufa; the basal slab and overlying thicker slabs showing natural horizontal splitting. Tufa is a type of limestone formed in calcareous springs.

Peiligang occupation

At Fudian (Liu *et al.* 2002-2004: Figure 3) pit fill and reference ash pit deposits contain local topsoil and subsoil materials, in addition to bone, burned bone, ash, charcoal, pottery, burned soil and phosphate materials indicating the disposal of human waste (Table 1, M34, 43 and 44). There is evidence in the ash pit of fine soil mobilization induced by the weathering of ash and the release of potassium (K), as also reported from Neolithic pits in Europe (Courty and Fedoroff 1982; Slager and Van der Wetering 1977).

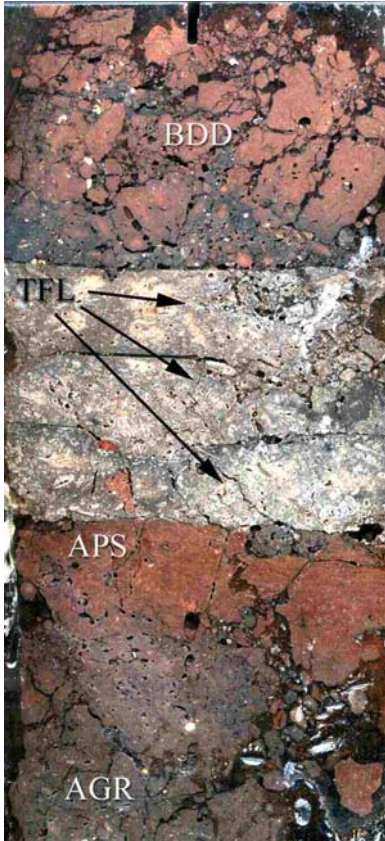


Figure 3: Scan of 14 cm long block (M19) that sampled Layer 7 – adobe ground-raising deposits (AGR) and plant-tempered adobe preparation surface (APS), Layer 8 – a series of fossiliferous tufa floor layer(s) (TFL), tufa slabs or slab showing natural horizontal splitting, and Layer 9 – burned daub (adobe) debris (BDD).

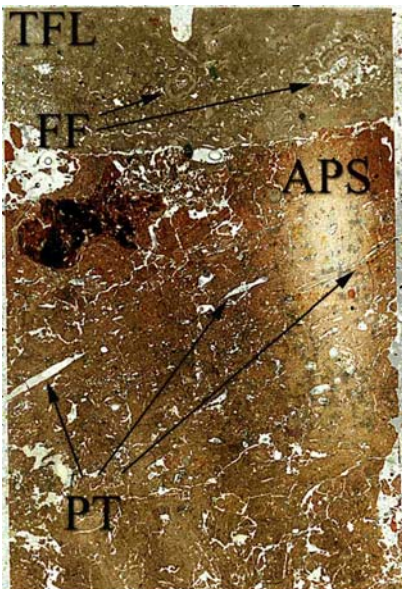


Figure 4: Scan of thin section M19B showing (Layer 7) voids pseudomorphic of plant-tempering (PT) and dark- coloured adobe preparation surface (APS) – a mud-plastered layer, and (Layer 8) tufa floor layers (TFL) containing fossil features (FF). Width is ~5cm.

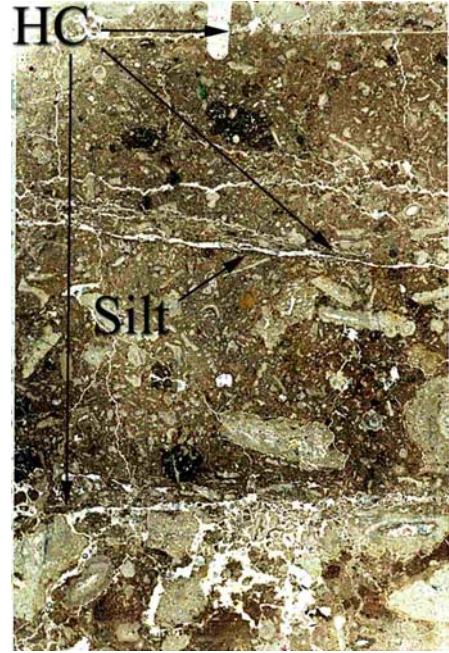


Figure 5: Scan of thin section M18A, tufa floor layers (Layer 6) containing loessic soil clasts and plant fossils, and showing horizontal cracks (HC) – natural horizontal splitting of the tabular tufa, and the location of fine-charcoal-rich loessic silt coating the base of one crack (Silt) – see text. Width is ~5cm.

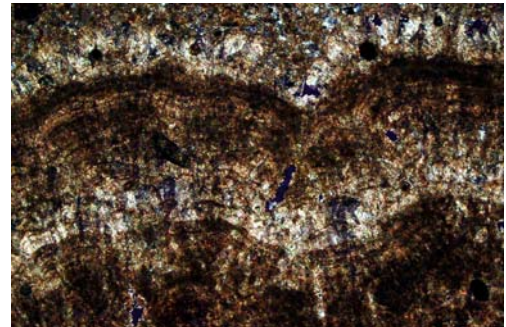


Figure 6: Photomicrograph of M1, fragmented sample of floor; detail of biochemical growth patterns in tufa. Crossed polarised light (XPL), frame width is ~2.3 mm.

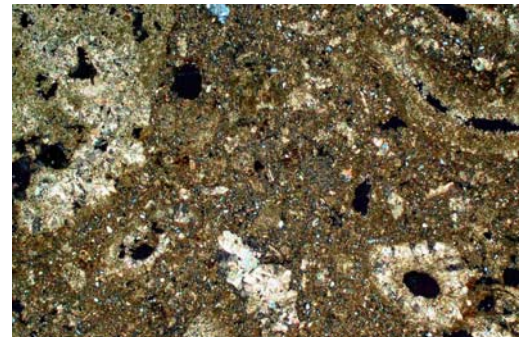


Figure 7: Photomicrograph of M18A, Floor Layer 6b, showing plant pseudomorphs and fossil remains formed by sparite (calcite) set in an impure micritic and microsparitic matrix (tufa) containing silt-size quartz (loess). XPL, frame width is ~4.6 mm.

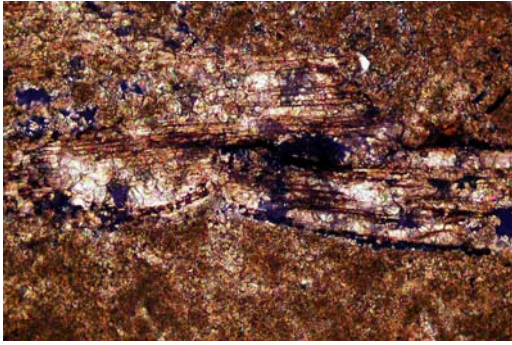


Figure 8: Photomicrograph of M18B, blackened plant tissues embedded in calcitic tufa as evidence of naturally included plant fragments. XPL, frame width is ~1.06 mm.

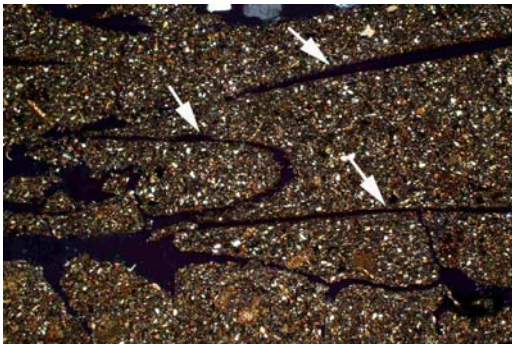


Figure 9: Photomicrograph of M18B, plant-tempered mud-plastered loess forming a floor preparation surface (arrows point out void pseudomorphs of plant tempering); the dense character of the matrix is due to soil slaking caused by the mud-plastering process. XPL, frame width is ~4.6 mm.

OCCUPATION AT HUIZUI

Off-site soil-sediments at GS2 (M39-40) and a floor sequence at 05HYEHF1 (Figure 1; M16A-M19B) were focused upon.

YANGSHAO FLOOR SEQUENCE 05HYEHF1

At this constructional sequence a number of layers (1-11) was examined (Figure 1). The floor sequence is broadly composed of four or more white floors laid on prepared surfaces (Tables 1 and 2). Layer 1 is composed of occupation soil (or ground-raising dump?) with a 2 mm thick compact, weakly layered soil spread immediately below the overlying white floor (Layer 2). This soil appears to be a 'plastered' soil layer and preparation surface, made from 'clean' loess. The white floor (Layer 2) is constructed from a 3 cm thick slab of fossiliferous tufa; in fact Layers 2, 4, 6 and 8 are all constructed from single or multiple 2-3 cm thick slabs of tufa that show natural horizontal splitting or jointing (see Figures 2-3). Bulk analysis of one example (Layer 8, Table 2) shows it to be highly calcareous (67.6% carbonate), but very impure (acid insoluble residue, 32.4%; mostly silts and clay), and has no signs whatsoever of phosphate enrichment or magnetic susceptibility enhancement. Soil micromorphology indicates that the silt and clay is present as included loess. Its sulphide content is also indicative of a natural water-

logged (gleyed) origin. Parallel elemental and mineralogical studies from this F1 floor sequence and the F4 floor at Huizui, found abundant calcite, with quartz, chlorite, illite and iron oxides/hydroxides, consistent with tufa forming alongside the inwash of loess (John Webb, La Trobe University, pers. comm., 2007).

Tufa as a constructional material

Tufa (cf. travertine) develops where spring water contains high amounts of dissolved calcium carbonate which precipitates as a mainly micritic limestone-like deposit. It also often forms around algae, lichens and mosses growing on site and produces pseudomorphs of plants in the form of microsparite- and sparite-size calcite, with some morphologies also reflecting the presence of bacteria and algae (Courty *et al.* 1989, 99, Figure 6.9b; Scholle and Scholle 2003: 349) (Figures 6-7). Tufa also often traps plant material and soil, at times, as found in the tufa floor slabs at Huizui (Figure 8). The presence of Quaternary tufa in the locality of Huizui is consistent with the weathering of loess and formation of calcium carbonate-rich Bk deep subsoil horizons and carbonate nodules in the area, and the likely formation of tufa associated with springs (cf. Avery 1990: 187-188). The ubiquitous presence of fossil traces of plants, organic remains and soil clasts, including both loess (see bulk analyses, above) and carbonate nodules, in the white floors, confirms their identification as quarried tufa slabs (Paul Goldberg, Boston University, pers. comm., 2006) (cf. Quaternary tufa-like beds in loess covered area of Kostenki, Russia; Holliday *et al.* 2007, Figure 6c). Although occasional burrowing by mesofauna is recorded in these floor layers, the fossil evidence cannot be mistaken for post-depositional rooting and secondary calcium carbonate formation, because such features do not cross boundaries between individual floor slabs of tufa (see Figures 2-3).

The natural splitting qualities of the tufa ('tabular formed tufa') presumably encouraged and aided quarrying. It is also evident that tufa slabs may also have been employed to create walls or partitions, as shown in Figure 1. (The complete absence of any chemical, mineralogical or micromorphological evidence of burning and the overwhelming indications of natural tufa formation demonstrate that none of the white floors investigated were manufactured from burned lime.)

Constructional sequence at 05HYEHF1 – layers 2-9

There is no evidence of occupation soils between floors, as for example formed when deposits are tracked-in by trampling, either by people or their animals (Macphail *et al.* 2004). This implies that either floors were swept and/or covered (Goldberg and Macphail 2006; Macphail *et al.* 1997; Matthews *et al.* 1996, 2000). Within floor Layer 6 (Figure 5) there is a rare example of very fine charcoal-rich silt deposition is recorded, but this may not be significant.

Instead of occupation deposits, soil Layer 3b between floor Layers 2 and 4b, is composed of unburned plant-tempered adobe (daub) manufactured from 'clean' loess

(sample 16/3b)(see Figures 4 and 9). The plant-tempering material has now been mainly lost through oxidation from this ground-raising construction level, as is typical of plant tempered adobe and mudbrick (Courty *et al.* 1989; Goldberg and Macphail 2006), and reference Yangshao burned daub (M33). The dark soil Layer (3a) below floor Layer 4a, was expected to be humic, but in fact is chemically very poorly humic and carries no anthropogenic signal (Table 2, samples 16/3a, 17/3a); again, it is simply composed of 'clean' loess. The dark colour has been produced by the manufacture of another mud 'plastered' surface; the soil when wetted, became slaked, causing the clay constituents to separate and infill voids, hence giving it a dark reddish colour (Figures 4 and 9) (Macphail and Goldberg 2006). Mud plastered surfaces have been recorded from numerous sites, including Çatalhöyük, Turkey and from ethnographic examples from Turkey and India (Boivin 1999; Matthews *et al.* 1996, 2000). Mud 'plastered' preparation levels (Layers 6 and 8; M18B and M19B) below floors are similarly plant-tempered adobe deposits (Figure 9). Layer 5 in the construction sequence was termed a yellowish clay in the field. In thin section, it is quite clear that this is a leveling dump that is mainly composed of pale soil from a presumably local A2 soil horizon of the local loess soil (see above).

Layer 9 which overlies floor Layer 8, is made up of coarse fragments of rubefied (moderately burned; see Table 1) daub and biologically worked fine pieces of unburned daub (M18A). The burned daub is probably associated with the burned daub wall of the structure that underlies floor layer 10 (Figures 1 and 3). This debris again rests on a clean floor surface. Such deposits could imply the razing of the structure by fire, as carried out experimentally at Butser Ancient Farm, Hampshire, UK or as found in London as the result of the revolt by Boudicca in AD59-60 (Goldberg and Macphail 2006: Figures 11.9 and 12.8; Macphail *et al.* 2004). In Neolithic China, however, daub walls are believed to have been burned (hardened) for constructional purposes (Chen, pers. comm. 2005).

Longshan ash pit 05HYEH3

Ash pit deposits (samples 10 and 11) are moderately humic in comparison to other contexts at Huizui, and are enriched or strongly enriched in phosphate. They also show an enhanced or strongly enhanced magnetic susceptibility. In thin section (M31A and M31B), they are characterized mainly by layered deposits of wood ashy material that include fine moderately strongly burned soil, and occasional charcoal, and laminated phytoliths, including articulated phytoliths (e.g., from plant processing and the dumping of 'mats'). (As yet there is no consensus on the use of the floors in the 05HYEHF1 sequence, but if they were domestic and as they are 'clean' this could be the result of having been covered with mats.) The wood ash is identifiable from large lozenge shape calcite crystals and wood charcoal present (Courty *et al.* 1989). The presence of human(?) coprolitic fragments, bone, pottery and probable amorphous Fe-Ca-P staining, indicate general dumping of food and latrine waste. Little biological activity is

recorded at these levels, possibly because of the high levels of alkali earths of ash origin that for example can be toxic to earthworms, and also because the layered character of the deposits is consistent with 05HYEH3 being an episodic ponded environment. Ephemeral waterlain occupation sediments in ditches, quarries, etc are not unusual in the archaeological record.

Longshan ash pit 05HYEH4

Chemically, this ash pit fill is similar to ash pit 05HYEH3, but records a more strongly enhanced magnetic susceptibility (samples 12 and 13). In the 150 mm sample examined in thin section (M22A and M22B) there are layers wood ash, mixed soil and long articulated phytoliths, and brown amorphous organic matter-stained layered articulated phytoliths. The last material is again believed to be from mats, but appear to be 'dirtier' than the 'mats' in 05HYEH3. There are recognizable phytoliths of grass stems, sedges and reeds (Rosen, pers. comm., 2006). The deposit was also affected by secondary iron staining and burrowing, and again may have developed under ponded conditions at times.

Yangshao and Longshan soil-sediment sequence at GS2 (05HYEGS2)

The section at GS2, comprises modern disturbed ground, below which there is a 2.30 m thick series of deposits (Table 1); this geological profile and others at lower and higher altitudes have been investigated by Rosen (this volume: Figures 2-4). In brief, at 0.20-0.45 m a massive and iron-stained layer containing a Longshan sherd, is capped by laminated beds, and these deposits were examined in samples 38a and 38b, and M38A and 38B. At around 2.00 metres fine weakly iron-stained deposits overlay a pale leached fine layer over gravel; the last contains Yangshao pottery (samples 39a and 39b, respectively; M39A, M39B, M39base and M39plan). This gravel apparently truncates an assumed natural Late Pleistocene/early Holocene alluvial soil, and the vertical junction between the two layers and the soil below were sampled (samples 40, M40A and 40B). A control sample of the lateral junction between laminated alluvium and the alluvial soil was also collected (M30) some 0.40 m distant. The characteristics of these soils and sediments are summarized in Table 2. Rooting is recorded in the lowermost grey alluvium which is devoid of anthropogenic material, unlike the Yangshao gravels and silty muds which overlie it. The latter contain sherds, sand to gravel size burned daub, carbonate nodules, tufa, bone, charcoal and phosphate nodules of anthropogenic origin (e.g., phosphate nodules that include of phytoliths and can be broadly termed as probable 'nightsoil' when of anthropogenic origin; Goldberg and Macphail 2006: 206). Due to post-depositional phosphate loss and groundwater movement (Thirly *et al.* 2006) phosphate is poorly recorded chemically, except for in sample 39a (Table 2) where secondary phosphate has apparently accumulated alongside iron and manganese (microprobe analysis). No enhancement in heavy metal concentrations was recorded,

however, in this sequence.

The Longshan samples (M38A and 38B) examined two gleyed layers where an apparently laminated deposit (38a) is present over a massive heterogeneous sediment (38b). The latter, includes large clasts of daub and burned daub (some with embedded charcoal), and smaller fragments of charcoal, fine bone and coprolite. Secondary iron-phosphate staining is present, and very dark, dusty clay void infills and coatings testify to the coarse turbation of this sediment under waterlogged conditions. The overlying and apparently laminated layer 39b, is equally rich in anthropogenic materials (daub, burned daub, bone, coprolite, charcoal, phosphate-stained charcoal-rich soil), but these are smaller and present as sand and coarse sand size material. In addition, occasional fine plant fragments, including 'soft' tissues, are present, and probably responsible for the highest LOI found in this sequence. On drying, however, the apparently laminated 'beds' have formed a lenticular structure. This, with the textural pedofeatures present that are again probably due to wet soil slaking and disturbance, suggest that a possible human trampled 'surface' layer formed in a waterlogged, fine anthropogenic sediment.

Erlitou contexts

A soil next to a well (sample 4), five ash pit deposits (samples 6-9, 14-15) and a 'road' (sample 37) were analysed. All deposits, with the exception of the soil, are enriched to very strongly enriched in phosphate-P (max. 13.3 mg g⁻¹ in sample 15, highest measured at Huizui) and show strong to very strong magnetic susceptibility enhancement, producing a marked anthropogenic signal.

The soil by the well appears to be a mainly truncated subsoil material (M4, fragments only) with little evidence of activity apart from some very dusty clay infills. The last could be the result of soil slaking induced by trampling and spillage of water.

An example of an ash pit (M8) shows a very heterogeneous and biologically mixed fill composed of soil, daub, burned daub, bone, coprolites, with very abundant charred and ashed plant material including millet (*in situ* phytolith evidence; Rosen, pers comm.). Several silica slag fragments of vitrified (vesicular voids) material are evidence of moderately high temperature burned phytoliths, consistent with the very strongly enhanced magnetic susceptibility (samples 6-9). These inclusions indicate that plant (cereal?) processing, kitchen and latrine (night-soil) waste have been dumped. The fill is not untypical of ash-rich deposits that have been studied in later prehistoric contexts in the UK (Macphail 2000; Macphail and Crowther 2002), but is less ash-rich compared with Longshan ash pits (see estimated carbonate in Table 2). M15 is wood ash dominated (excavated 'white layer') and charred bark is present; the included strongly burned soil, daub, and cess also contribute to the strong phosphate and magnetic susceptibility signal.

The 'road' sediment is very compact and although it includes coarse burned daub, much of the anthropogenic material is fine sand to medium sand-size; shell, charcoal,

bone, rubefied burned bone, probably phosphate-cemented bone rich aggregates (nightsoil) are present and contribute to the anthropogenic phosphate and magnetic susceptibility signal (sample 37). The fine-sorting is typical of trampled surfaces, and pseudolayering is expressed by charred organic matter and planar voids relict of oxidized plant remains that were horizontally oriented. From experiments and analysis of occupation surfaces, such deposits can develop by human trampling producing a beaten surface under relatively dry conditions; in the UK this was within roofed structures (Goldberg and Macphail 2006; Macphail *et al.* 2004). Here it is a 'beaten track'. Other layers within this road, however, show the development of dusty clay panning and clay void infills that more likely relate to passage when the road was muddy (Rentzel and Narten 2000).

CONCLUSIONS

Although 31 thin sections and 25 bulk samples were investigated from in and around Huizui after fieldwork in 2005, site interpretations are still at an early stage and need to be treated with caution. Soil micromorphology (with microprobe) was combined with analyses of LOI, fractionated phosphate, magnetic susceptibility including χ_{\max} , and the heavy metals Cu, Pb and Zn to produce a preliminary understanding of the microstratigraphy of soils and sediments from the Peiligang to Erlitou Periods. This produced a broad, albeit limited, dataset, which has allowed this article to focus upon our understanding of the constructional origins of a Yangshao floor sequence. Here, ground-raising was carried out using plant-tempered adobe manufactured from local 'clean' loess soils, with mud-plastered surfaces creating dark 'red' layers immediately below each white floor. The white floors themselves are not manufactured burned lime floors, but constructed from single to multiple slabs of tufa that may well have been quarried locally from tabular tufa formed along spring lines. Such slabs appear to be in excess of 3-4 m in size, the quarrying and transport of which imply a high degree of social organization. No quarries have yet been identified, however. No Yangshao occupation floor deposits were found (only ground-raising deposits), suggesting that either floors were of ritual use (Liu, pers. comm.) or were swept or mat-covered. The overall dataset also provides punctuated insights into the occupational and landscape history of the site, including likely manipulation of the fluvial system and the 'off-site' marked accumulation of anthropogenic soils and sediments under water-logged conditions.

ACKNOWLEDGEMENTS

The authors thank their chief co-workers at Huizui (Li Liu and John Webb, La Trobe University, Australia; Xingcan Chen, Institute of Archaeology, Chinese Academy of Social Sciences, China; and Arlene Rosen, University College London) for their collaboration and discussion, and gratefully acknowledge the Australian Research Council grant that supported this study. John Webb (La Trobe University) kindly allowed us to cite his mineralogical

data. The authors also thank Gyoung-Ah Lee and Ming Wei (La Trobe University) for their assistance during fieldwork. Paul Goldberg's (Department of Archaeology, Boston University) comments on some of the thin sections are also gratefully acknowledged, as are the observations of Chris Hayward (Department of Geology, University of Cambridge).

REFERENCES

- Avery, B.W. 1990. *Soils of the British Isles*: Wallingford, CAB International.
- Bethell, P.H. and I. Máté. 1989. The use of soil phosphate analysis in archaeology: A critique. In J. Henderson (ed.), *Scientific Analysis in Archaeology*, 19, pp. 1-29. Oxford: Oxford University Committee.
- Boivin, N.L., 1999. Life rhythms and floor sequences: excavating time in rural Rajasthan and Neolithic Çatalhöyük. *World Archaeology* 31: 367-388.
- Bouma, J., C.A. Fox, and R. Miedema. 1990. Micromorphology of hydromorphic soils: applications for soil genesis and land evaluation. In Douglas, L.A. (ed.) *Soil Micromorphology: A Basic and Applied Science*, 19 *Developments in Soil Science*, pp 257-278. Amsterdam: Elsevier.
- Courty, M.A., and N. Fedoroff. 1982. Micromorphology of a Holocene dwelling, Proceedings Nordic Archaeometry, *PACT* 7: 257-277.
- Courty, M.A., P. Goldberg and R.I. Macphail. 1989. *Soils and Micromorphology in Archaeology*. Cambridge: Cambridge University Press.
- Crowther, J. 2003. Potential magnetic susceptibility and fractional conversion studies of archaeological soils and sediments. *Archaeometry* 45: 685-701.
- Crowther, J., and P. Barker. 1995. Magnetic susceptibility: distinguishing anthropogenic effects from the natural. *Archaeological Prospection* 2: 207-215.
- Duchaufour, P. 1982. *Pedology*. London: Allen and Unwin.
- FAO-Unesco. 1988. *Soil Map of the World*. Rome: FAO.
- Goldberg, P. and R.I. Macphail. 2006. *Practical and Theoretical Geoarchaeology*. Oxford: Blackwell Publishing.
- Holliday, V.T., Hoffecker, J., Goldberg, P., Macphail, R.I., Forman, S., Anikovich, M.V. and Sinitsyn, A.A. 2007. Geoarchaeology of the Kostenki-Borshchevo sites, Don River Valley, Russia. *Geoarchaeology* 22: 181-228.
- Liu, L., X. Chen, Y.K. Lee, H. Wright and A. Rosen. 2002-2004. Settlement patterns and developing of social complexity in the Yiluo Region, north China. *Journal of Field Archaeology* 29: 75-100.
- Macphail, R.I. 2000. Soils and microstratigraphy: a soil micromorphological and micro-chemical approach. In A.J. Lawson (ed.), *Potterne 1982-5: Animal Husbandry in Later Prehistoric Wiltshire*, 17 *Archaeology Report*, pp 47-70. Salisbury: Wessex Archaeology.
- Macphail, R.I., Courty, M.A., Hather, J., and Watzet, J., 1997. The soil micromorphological evidence of domestic occupation and stabling activities. In R. Maggi (ed.), *Arene Candide: a Functional and Environmental Assessment of the Holocene Sequence (Excavations Bernabò Brea-Cardini 1940-50)*, pp 53-88. Roma: Memorie dell'Istituto Italiano di Paleontologia Umana.
- Macphail, R.I., and J. Crowther. 2002. *Battlesbury, Hampshire: soil micromorphology and chemistry (W4896)*. Unpublished report, Salisbury: Wessex Archaeology.
- Macphail, R.I., and J. Crowther. 2004. Tower of London Moat: sediment micromorphology, particle size, chemistry and magnetic properties. In G. Keevil (ed.), *Tower of London Moat Excavation, 1 Historic Royal Palaces Monograph*, pp 41-43, 48-50, 78-79, 82-83, 155, 183-186, 202-204 and 271-284. Oxford: Oxford Archaeology.
- Macphail, R.I., G.M. Cruise, M.J. Allen, J. Linderholm and P. Reynolds. 2004. Archaeological soil and pollen analysis of experimental floor deposits; with special reference to Butser Ancient Farm, Hampshire, UK. *Journal of Archaeological Science* 31: 175-191.
- Matthews, W., C.A.I. French, T. Lawrence and D. Cutler. 1996. Multiple Surfaces: the Micromorphology. In I. Hodder (ed.), *On the Surface: Çatalhöyük 1993-95*, pp 301-342. Cambridge: McDonald Institute for Archaeological Research and British Institute of Archaeology at Ankara.
- Matthews, W., C.A. Hastorf and B. Ergenekon. 2000. Ethnoarchaeology: studies in local villages aimed at understanding aspects of the Neolithic site. In I. Hodder (ed.), *Towards Reflexive Method in Archaeology: the Example at Çatalhöyük*, pp 177-188. Cambridge: McDonald Institute for Archaeological Research and British Institute of Archaeology at Ankara.
- Rentzel, P., and G.-B. Narten. 2000. Zur Entstehung von Gehniveaus in sandig-lehmigen Ablagerungen - Experimente und archäologische Befunde (Activity surfaces in sandy-loamy deposits - experiments and archaeological examples), *Jahresbericht 1999*, pp 107-27. Basel: Archäologische Bodenforschung des Kantons Basel-Stadt.
- Slager, S., and H.T.J. Van der Wetering. 1977. Soil formation in archaeological pits and adjacent loess soils in Southern Germany. *Journal of Archaeological Science* 4: 259-67.
- Soil Survey Staff. 1999. *Soil Taxonomy*. Washington D. C.: U. S. Department of Agriculture, U. S. Government Printing Office.
- Stoops, G. 2003. *Guidelines for Analysis and Description of Soil and Regolith Thin Sections*. Madison, Wisconsin: Soil Science Society of America, Inc.
- Thirly, M., J. Galbois, and J.-M. Schmitt. 2006. Unusual phosphate concretions related to groundwater flow in a continental environment. *Journal of Sedimentary Research*, 76: 866-877.

Table 1: Huizui soil micromorphology (thin section) and bulk samples; preliminary interpretations (continued on next page)

Site Code	Bulk analysis (Table 2)	Period and Context	Thin section (relative depth); preliminary interpretation
Qijiyao		Peiligang soil and pits	
05HYQGS2	43	Subsoil A2&Bt? Horizon	M43 0-75 mm: Deep loessic A2 soil horizon with rare bioworked fine charcoal throughout.
05HYQH1	44	Pit 1 - lower part near large shell	M44 0-75 mm: Loessic soil- (A2, Bt and calcareous Btk horizon) dominated fill with burned soil, pottery, charcoal, bone, and phosphate features indicative of disposal of human waste.
(Fudian)		Peiligang fused ash	M34 reference sample: Wood ash, recemented (partially weathered) ash, burned bone, soil and burned soil.
Huizui		Yangshao F1 floor sequences	
05HYEHF1		Layer 9: burned clay	M19A 0-75 mm: Burrowed fragments of burned daub presumed to be relict of burned adobe (daub) construction (red coloured because of both soil slaking and moderate burning).
05HYEHF1	19/8	Layer 8: floor	M19A 0-75 mm (M19B): 2 tufa slabs, with plant pseudomorphs and plant remains, loess soil inclusions and staining. (high carbonate content; absence of magnetic susceptibility enhancement) (Parallel mineralogical studies* of floor slabs found quartz, chlorite, illite and iron oxide/hydroxides, consistent with the presence of loess).
05HYEHF1		Upper layer 7: floor preparation material?	M19B 75-150 mm: Mud plastered layer constructed from plant-tempered loess over loess-based plant-tempered adobe.
05HYEHF1		Layers 6a and 6b: uppermost and middle floor layer of floor series	M18A 10-85 mm: 2-3 tufa slabs, with very thin (charcoal) fine dusty clay surface layer between middle (6b) and uppermost (6a) layers.
05HYEHF1		Layer 6c: lowermost floor of floor series	M18B 85-140 mm: two tufa slabs.
05HYEHF1		Layer 6d: floor preparation material	M18B 140-170 mm: Mud plastered layer constructed from plant-tempered loess
05HYEHF1		Layer 5: yellowish clay leveling/ground-raising deposit	Probable pale A2 horizon soil, as in M17A below.
05HYEHF1	17/4a	Layer 4a: dark fill	M17A 0-55 mm: ground-raising mixture of pale A2 horizon soil and burned daub (hence enhanced magnetic susceptibility).
05HYEHF1		Layer 4b: floor	M17B 95-105 mm: tufa slab (basal slab of three).
05HYEHF1	17/3a	Layer 3a: dark brown - floor preparation deposit	M17B 105-115 mm: Mud plastered layer constructed from loess; dark colour formed by the slaking of the loess and formation of clay textural pedofeatures features (no bulk evidence of added humic matter)
05HYEHF1		Layer 3b:	M17B 115-165 mm: Adobe ground-raising deposit constructed from 'clean' loess.
05HYEHF1	16/3a	Layer 3a: brown - floor preparation deposit (lateral continuation of 17/3a)	No bulk signal of anthropogenic deposition or humic soil formation.
05HYEHF1	16/3b	Layer 3b: floor fill	No bulk signal of anthropogenic deposition or humic soil formation.
05HYEHF1		Layer 2: floor	M16A 0-5 mm: Floor constructed of a single slab of quarried tufa. M16B 5-75 mm: Thin plant-tempered 'mud-plastered' floor preparation surface made from loess (adobe), over occupation soil with enriched phosphate-P and enhanced magnetic susceptibility.
05HYEHF1	16/1	Layer 1: disturbed soil/deposit	M16B 80-155 mm: occupation soil, as above.
05HYHF1		Fragmented sample of floor	M1: Three coarse fragments of tufa ('floor')
05HYHF1		Floor	M2 0-30 mm: Floor constructed of quarried slab of tufa, over; 30-35 mm: plant-tempered 'mud-plastered' floor preparation surface composed of 'clean' loess.
05HYEH3		Longshan ash pit	
05HYEH3S1	10	Ashpit	M31A 0-75 mm: Pit (quarry?) fill of likely ponded deposits composed of layered occupation soil, wood ash, and phytolith remains of plants; the last probably reflects inputs of cereal and plant processing waste and mats. Inputs of human cess and inwash of iron, calcium and phosphate under episodic wet conditions.
05HYEH3S2	11	Ashpit	M31B 75-150 mm: as above
05HYEH3		Mixed occupation soil below ash layers	M32 0-75 mm: Basal pit (quarry?) fill of disturbed topsoil and subsoil, and burrowed occupation deposits from overlying fill; inwash of iron, calcium and phosphate under episodic wet conditions.
05HYEH4		Longshan ash pit	
05HYH4S1	12	Series of thin ash and charcoal layers	M22A 0-75 mm: Very similar to ash pit fill H3 (see above), but includes more strongly burned materials, and 'mat' residues appear to include more fine anthropogenic inclusions ('dirtier?').
05HYH4S2	13	Series of thin ash and charcoal layers	M22B 75-150 mm: as above
		Holocene, Yangshao and Longshan soil-sediment sequence at GS2	(see overleaf)

05HYEGS2	38a	Longshan fine laminated alluvium - flood deposits?	M38A 0-55 mm: Lenticular structured possible human trampled wet, gleyed anthropogenic sediment, containing many fine anthropogenic inclusions.
05HYEGS2	38b	Longshan soil-sediment with vertically oriented sherd	M38A 55-75 mm: as below M38B 75-150 mm: Massive, coarsely churned, wet, gleyed anthropogenic sediment, containing many coarse anthropogenic inclusions.
05HYEGS2	39a	Yangshao soil-sediment towards base of soil-sediment sequence	M39A 0-75 mm: massive silts with iron and manganese staining; occasional fine included anthropogenic material (probable post-depositional phosphate-enriched, along with Fe-Mn). M39plan: ditto, and as demonstrated by microprobe.
05HYEGS2	39b	Yangshao gravel deposits at base of soil-sediment sequence	M39B 75-150 mm: poorly laminated, silty muds with detrital organic matter fragments (75-100 mm), over unsorted gravel-rich fill containing rounded burned daub, and calcium carbonate-rich subsoil and tufa, with loess, charcoal and sand to silt size bone and phosphate nodules of anthropogenic origin (100-150 mm). M39base 0-75 mm: same sequence
05HYEGS2	40	Late Pleistocene/early Holocene(?) alluvial soil	M40A 0-75 mm: Gravel (0-15 mm) over (truncating?) uppermost part of soil (see below). M40B 75-150 mm: Late Pleistocene/early Holocene(?) alluvial gley soil formed from redeposited loess, with iron stained root channels and containing no anthropogenic inclusions.
05HYEGS2		Laminated Holocene (Yangshao?) alluvium abutting truncated Late Pleistocene/Early Holocene soil	M30 0-75 mm: finely laminated silty alluvium abutting Late Pleistocene/early Holocene alluvial gley soil formed from redeposited loess, with iron stained root channels and containing no anthropogenic inclusions.
		Erlitou soil, ash pits and 'road'	
04HYHT4J1	4	Surface by well	M4 (fragments only): A truncated subsoil with indications of trampling and water spillage.
05HYHWTer2 H2	8 and 9 (6 and 7)	Ashpit 2 deposits	M8 0-75 mm: Strongly phosphate-enriched ash pit deposit containing very strongly burned materials (vitrified silica slags), ash, plant processing and human coprolites/cess.
T3H22	15	Erlitou Phase III Ashpit deposit	M15 (fragments only): ash- (wood ash) dominated, with strongly burned soil, daub, and cess, all resulting in the highest phosphate concentrations and the highest magnetic susceptibility (% χ conv) at Huizui.
05HYHWTer2 L1	37	Erlitou 'road'	M37 0-75 mm: compact, partially layered trampled soil containing many mainly fine anthropogenic inclusions, and formed under both wet and 'dry' conditions.

* Mineralogical studies by Dr John Webb, La Trobe University.

Table 2: Huizui chemical (excluding phosphate fractionation) and magnetic susceptibility data (continued on next page)

Sample	Brief description	LOI (%)	pH 1:2.5 water	Carbonate (est, %) \S	Phosphate-P \ddagger (mg g $^{-1}$)	Pb $\$$ (mg g $^{-1}$)	Zn $\$$ (mg g $^{-1}$)	Cu $\$$ (mg g $^{-1}$)	χ (10 $^{-8}$ SI)	χ max (10 $^{-8}$ SI)	χ conv \parallel (%)
Peiligang soil and pits (Qijiayao; 05HYQ and 05HYQGS2)											
43	Subsoil A2&Bt?	1.08	8.6	5	0.871				23.8	298	7.99*
44	Pit 1	1.30	8.2	2	1.26				34.8	355	9.80*
Yangshao floor and construction sequence											
17/4a	Floor: Layer 4a	1.26	8.5	5	2.46				53.0	877	6.04*
17/3a	Floor: Layer 3a	0.782	8.8	>10	1.30	18.4	40.6	14.8	20.3	880	2.31
16/3a	Floor: Layer 3a	0.984	8.8	5	1.25				18.0	1000	1.80
16/3b	Floor: Layer 3b	1.09	8.7	5	1.29				22.3	911	2.45
16/1	Pre-floor: Layer 1	1.44	8.7	>10	3.13*	17.0	68.2	25.6	37.8	522	7.24*
Longshan ash pits											
10	Ash pit	2.25	8.6	5	7.24**				27.4	144	19.0**
11	Ash pit	2.13	8.7	>10	4.98*				16.4	179	9.16*
12	Ash pit	2.37	9.6	>10	5.21**				59.6	256	23.3***
13	Ash pit	1.99	9.6	>10	5.94**				68.7	294	23.4***
Yangshao (Y) and Longshan (L) soil-sediment sequence at GS2 (05HYEGS2)											
38a	Alluvium (L)	1.76	9.4	>10	1.25	24.4	75.1	22.5	12.1	433	2.79
38b	Soil (L)	1.08	9.6	>10	1.90	20.0	60.0	20.0	9.7	269	3.61
39a	Basal soil (Y)	1.14	9.6	>10	3.59*	16.7	42.6	14.8	19.7	447	4.41

39b	Underlying gravel (Y)	1.25	9.4	>10	0.801	16.6	47.6	16.6	9.8	390	2.51
40	Underlying alluvial soil	1.04	9.1	5	1.07	18.8	50.1	18.8	10.3	542	1.90
Erlitou soil, ash pits, 'road' and floors											
4	Surface by well	1.08	8.3	>10	1.32				28.1	576	4.88
6	Ash pit	3.44	8.2	2	6.89**				103	309	33.3***
7	Ash pit	2.43	8.4	5	5.40**				192	462	41.6***
8	Ash pit	2.76	8.3	2	7.12**				56.6	255	22.2***
9	Ash pit	2.84	8.2	5	5.55**				99.4	331	30.0***
37	'Road'	1.61	8.6	5	3.54*				140	744	18.8**
14	Upper ash pit layer	1.98	8.6	>10	11.6***				164	406	40.4***
15	Lower ash pit layer	1.51	8.7	>10*	13.3***				142	279	50.9***

§ **Estimated carbonate:** * figure highlighted in bold appears to have a higher carbonate content than the other samples recorded as >10%, ** based on acid insoluble residue determination for this sample (AIR = 32.4%).

† **Phosphate-P:** Figures highlighted in bold show signs of phosphate-P enrichment: * = enriched (2.50-4.99 mg g⁻¹), ** = strongly enriched (5.00-9.99 mg g⁻¹), *** = very strongly enriched (≥10.0 mg g⁻¹) – phosphate fractionation data are presented in Table 3.

§ **Heavy metals (Pb, Zn & Cu):** None of the samples analysed shows clear signs of enrichment.

† **χ:** Figures highlighted in bold show signs of magnetic susceptibility enhancement: * = enhanced (χ_{conv} = 5.00-9.99%), ** = strongly enhanced (χ_{conv} = 10.0-19.9%), *** = very strongly enhanced (χ_{conv} ≥20.0%).